Since January 2020 Elsevier has created a COVID-19 resource centre with free information in English and Mandarin on the novel coronavirus COVID-19. The COVID-19 resource centre is hosted on Elsevier Connect, the company's public news and information website.

Radiological findings from 81 patients with COVID-19 pneumonia in Wuhan, China: a descriptive study

Heshui Shi, Xiaoyu Han*, Nanchuan Jiang*, Yukun Cao, Osamah Alwalid, Jin Gu, Yanqing Fan†, Chuansheng Zheng†*

Summary

Background **A cluster of patients with coronavirus disease 2019 (COVID-19) pneumonia caused by infection with severe acute respiratory syndrome coronavirus 2 (SARS-CoV-2) were successively reported in Wuhan, China. We aimed to describe the CT findings across different timepoints throughout the disease course.**

Methods **Patients with COVID-19 pneumonia (confirmed by next-generation sequencing or RT-PCR) who were admitted to one of two hospitals in Wuhan and who underwent serial chest CT scans were retrospectively enrolled. Patients were grouped on the basis of the interval between symptom onset and the first CT scan: group 1 (subclinical patients; scans done before symptom onset), group 2 (scans done ≤1 week after symptom onset), group 3 (>1 week to 2 weeks), and group 4 (>2 weeks to 3 weeks). Imaging features and their distribution were analysed and compared across the four groups.**

Findings **81 patients admitted to hospital between Dec 20, 2019, and Jan 23, 2020, were retrospectively enrolled. The cohort included 42 (52%) men and 39 (48%) women, and the mean age was 49·5 years (SD 11·0). The mean number of involved lung segments was 10·5 (SD 6·4) overall, 2·8 (3·3) in group 1, 11·1 (5·4) in group 2, 13·0 (5·7) in group 3, and 12·1 (5·9) in group 4. The predominant pattern of abnormality observed was bilateral (64 [79%] patients), peripheral (44 [54%]), ill-defined (66 [81%]), and ground-glass opacification (53 [65%]), mainly involving the right lower lobes (225 [27%] of 849 affected segments). In group 1 (n=15), the predominant pattern was unilateral (nine [60%]) and multifocal (eight [53%]) ground-glass opacities (14 [93%]). Lesions quickly evolved to bilateral (19 [90%]), diffuse (11 [52%]) ground-glass opacity predominance (17 [81%]) in group 2 (n=21). Thereafter, the prevalence of ground-glass opacities continued to decrease (17 [57%] of 30 patients in group 3, and five [33%] of 15 in group 4), and consolidation and mixed patterns became more frequent (12 [40%] in group 3, eight [53%] in group 4).**

Interpretation **COVID-19 pneumonia manifests with chest CT imaging abnormalities, even in asymptomatic patients, with rapid evolution from focal unilateral to diffuse bilateral ground-glass opacities that progressed to or co-existed with consolidations within 1–3 weeks. Combining assessment of imaging features with clinical and laboratory findings could facilitate early diagnosis of COVID-19 pneumonia.**

Funding **None.**

Lancet Infect Dis 2020; 20: 425–34

Published Online February 24, 2020 https://doi.org/10.1016/S1473-3099(20)30086-4

See Comment page 384

For the Chinese translation of the abstract see Online for appendix 1

*Contributed equally

†Contributed equally

Department of Radiology, Union Hospital, Tongji Medical College, Huazhong University of Science and Technology, Wuhan, Hubei, China (H Shi MD, X Han MD, N Jiang MD, Y Cao MD, O Alwalid MD, J Gu MD, Prof C Zheng MD); **Hubei Province Key Laboratory of Molecular Imaging, Wuhan, Hubei, China** (Prof H Shi, X Han, N Jiang, Y Cao, O Alwalid, J Gu, Prof C Zheng); **Department of Radiology, Wuhan Jinyintan Hospital, Wuhan, Hubei, China** (Y Fan MD)

Correspondence to:
Dr Yanqing Fan, Department of Radiology, Wuhan Jinyintan Hospital, Wuhan, Hubei 430022, China
1024932023@qq.com

or

Prof Chuansheng Zheng, Department of Radiology, Union Hospital, Tongji Medical College, Huazhong University of Science and Technology, Wuhan, Hubei 430022, China
hqzcsxh@sina.com

Introduction

Beginning in December, 2019, a cluster of cases of pneumonia with unknown cause was reported in Wuhan, in the Hubei province of China.[1] On Jan 7, 2020, a novel coronavirus, severe acute respiratory syndrome coronavirus 2 (SARS-CoV-2; previously known as 2019-nCoV), was identified as the causative organism by Chinese facilities via deep sequencing analysis of patients' respiratory tract samples.[2,3] SARS-CoV-2 has been shown to infect human respiratory epithelial cells through an interaction between the viral S protein and the angiotensin-converting enzyme 2 receptor on human cells; thus, SARS-CoV-2 possesses a strong capability to infect humans.[3]

Most of the initial cases of coronavirus disease 2019 (COVID-19), the disease caused by SARS-CoV-2, were epidemiologically linked to exposure to Wuhan's Huanan seafood market, where wild animals are traded.[4,5] Although the market has been closed since Jan 1, 2020, as part of efforts to contain the outbreak, patients without exposure to the market but with a history of travel to Wuhan or close physical contact with a patient confirmed to have COVID-19, including health-care workers, have also been identified, suggesting strong human-to-human transmission. The number of cases has been increasing rapidly: by Feb 15, 2020, more than 60 000 cases of COVID-19 pneumonia had been reported in China and in other countries worldwide (including Thailand, Japan, South Korea, and the USA),[6–9] and 1524 patients had died, equivalent to a mortality rate of around 2%.

The clinical features of the initial 41 patients confirmed to be infected with SARS-CoV-2 included lower respiratory tract illness with fever, dry cough, and dyspnoea,[5] a manifestation similar to those of two other diseases caused by coronaviruses, severe acute respiratory syndrome (SARS) and Middle East respiratory syndrome (MERS).[10,11] However, the radiological changes in the lungs of people with COVID-19 pneumonia have not

Research in context

Evidence before this study

Before this study, we searched PubMed, Medline, and Google Scholar on Jan, 24, 2020, for articles describing the radiological features of patients infected with severe acute respiratory syndrome coronavirus 2 (SARS-CoV-2; previously known as 2019 novel coronavirus [2019-nCoV]), using the search terms "novel coronavirus" or "2019-nCoV" and "radiology "or "imaging" or "CT", with no time restrictions. We also searched CNKI and Wanfang Data using the same terms in Chinese, with no time restrictions. We found only previously published research discussing the radiological characteristics of severe acute respiratory syndrome coronavirus or Middle East respiratory syndrome coronavirus, and preliminary studies on the evolution of SARS-CoV-2 in Wuhan. We found no published work about the radiological characteristics of patients with pneumonia caused by SARS-CoV-2 infection.

Added value of this study

We analysed chest CT images from 81 patients confirmed to have COVID-19 pneumonia caused by SARS-CoV-2 infection, and described the imaging findings across different follow-up periods of the disease, including subclinical and clinical stages up to 3 weeks after symptom onset. This study is, to the best of our knowledge, the largest case series to date on the CT findings of COVID-19 pneumonia worldwide, and provides detailed information on the radiological, clinical, and laboratory features of these patients. Our findings provide insight in the evolution of the disease and its corresponding imaging changes, and suggest potential associations between imaging findings and patient outcomes, which requires further study.

Implications of all the available evidence

SARS-CoV-2 has substantial capacity to infect humans, and is capable of human-to-human transmission. Infection can lead to severe respiratory symptoms, including acute respiratory distress syndrome, and the mortality rate is around 2%. Combining imaging assessments with clinical and laboratory findings could help to identify SARS-CoV-2 infections early.

been fully characterised. CT is important in the diagnosis and treatment of lung diseases. In our experience, the imaging features of COVID-19 pneumonia are diverse, ranging from normal appearance to diffuse changes in the lungs. In addition, different radiological patterns are observed at different times throughout the disease course. Because the time between onset of symptoms and the development of acute respiratory distress syndrome (ARDS) was as short as 9 days among the initial patients with COVID-19 pneumonia,[5] early recognition of the disease is essential for the management of these patients.

We aimed to analyse the evolution of chest CT imaging features in patients with COVID-19 pneumonia, and to compare the imaging findings across the disease course, to facilitate early diagnosis of this newly emerging, life-threatening infection.

Methods

Study design and participants

This was a retrospective study done at two centres in Wuhan. Patients with confirmed COVID-19 pneumonia who were admitted to Wuhan Jinyintan hospital or Union Hospital of Tongji Medical College, and who underwent serial chest CT scans, were retrospectively enrolled.

In the patients who presented to Wuhan Jinyintan Hospital, SARS-CoV-2 infection was confirmed by next-generation sequencing or real-time RT-PCR, in according with a previously published protocol.[5] The following primers and probe targeted to the envelope gene of SARS-CoV-2 were used: forward primer 5′-TCAGAATGCCAATCTCCCCAAC-3′; reverse primer 5′-AAAGGTCCACCCGATACATTGA-3′; probe 5′CY5-CTAGTTACACTAGCCATCCTTACTGC-3′BHQ1.

The diagnosis of the cases from Union Hospital was initially based on the criteria published by WHO on Jan 12, 2020,[12] and all cases were later confirmed by real-time RT-PCR analysis of throat swab specimens, using the same protocol as above when PCR kits were available.

Based on the time interval between onset of symptoms and the CT scan, we designated four groups of patients in our study: group 1 (subclinical cases, in which CT scans were done before onset of symptoms); group 2 (CT scans done ≤1 week after symptom onset); group 3 (CT scans done >1 to 2 weeks after symptom onset); and group 4 (CT scans done >2 weeks to 3 weeks after symptom onset). Three readers (XH, NJ, and YF) recorded the clinical characteristics, laboratory findings, and comorbidities of the patients at the time of imaging.

This study was approved by the institutional review boards of the relevant centres. The requirement for informed patient consent was waived by the ethics committee for this retrospective study.

CT image acquisition

All CT scans were obtained with patients in the supine position, using one of the following scanners: SOMATOM Perspective, SOMATOM Spirit, or SOMATOM Definition AS+ (Siemens Healthineers, Forchheim, Germany). Scans were done from the level of the upper thoracic inlet to the inferior level of the costophrenic angle, and the following parameters were used: detector collimation widths 64 ×0·6 mm, 128×0·6 mm, 64×0·6 mm, and 64×0·6 mm; and tube voltage 120 kV. The tube current was regulated by an automatic exposure control system (CARE Dose 4D; Siemens Healthineers). Images were reconstructed with a slice thickness of 1·5 mm or 1 mm and an interval of 1·5 mm or 1 mm, respectively. The

	All patients (n=81)	Group 1 (n=15)	Group 2 (n=21)	Group 3 (n=30)	Group 4 (n=15)	p value*
Characteristics						
Age, years	49·5 (11·0)	44·9 (9·0)	48·8 (13·0)	52·3 (13·0)	49·5 (11·0)	0·2778
>50	40 (49%)	4 (27%)	10 (48%)	19 (63%)	7 (47%)	0·1444
≤50	41 (51%)	11 (73%)	11 (52%)	11 (37%)	8 (53%)	..
Sex	..	..	..	..	..	0·0871
Male	42 (52%)	4 (27%)	11 (52%)	20 (67%)	7 (47%)	..
Female	39 (48%)	11 (73%)	10 (48%)	10 (33%)	8 (53%)	..
History of exposure to Huanan market	31 (38%)	0	8 (38%)	14 (47%)	9 (60%)	0·0013
Symptoms						
Fever	59 (73%)	0	18 (86%)	27 (90%)	14 (93%)	<0·0001
Maximum temperature, °C	..	36·6 (0·1)	38·1 (0·8)	38·2 (0·8)	38·5 (0·7)	<0·0001
≤37·3	24 (30%)	15 (100%)	3 (14%)	5 (17%)	1 (7%)	<0·0001
37·3–38	20 (25%)	0	9 (43%)	8 (27%)	3 (20%)	..
38–39	23 (28%)	0	7 (33%)	11 (37%)	5 (33%)	..
>39	14 (17%)	0	2 (10%)	6 (20%)	6 (40%)	..
Dyspnoea	34 (42%)	0	9 (43%)	13 (43%)	12 (80%)	<0·0001
Chest tightness	18 (22%)	0	5 (24%)	7 (23%)	6 (40%)	0·0467
Cough	48 (59%)	0	15 (71%)	21 (70%)	12 (80%)	<0·0001
Sputum	15 (19%)	0	3 (14%)	6 (20%)	6 (40%)	0·0385
Rhinorrhea	21 (26%)	0	5 (24%)	10 (33%)	6 (40%)	0·0279
Anorexia	1 (1%)	0	1 (5%)	0	0	0·6296
Weakness	7 (9%)	0	1 (5%)	4 (13%)	2 (13%)	0·4065
Vomiting	4 (5%)	0	2 (10%)	2 (7%)	0	0·5777
Headache	5 (6%)	0	2 (10%)	2 (7%)	1 (7%)	0·8645
Dizziness	2 (2%)	0	0	1 (3%)	1 (7%)	0·8056
Diarrhoea	3 (4%)	0	1 (5%)	1 (3%)	1 (7%)	1·0000
Laboratory results						
Leukocyte count, ×10⁹/L	8·1 (3·4)	8·0 (2·5)	7·8 (3·6)	8·4 (3·5)	8·2 (4·2)	0·9337
<10	55 (68%)	12 (80%)	14 (67%)	19 (63%)	10 (67%)	0·7647
≥10	26 (32%)	3 (20%)	7 (33%)	11 (37%)	5 (33%)	..
Lymphocyte count, ×10⁹/L	1·1 (0·3)	1·1 (0·3)	1·0 (0·3)	1·1 (0·3)	1·1 (0·3)	0·8557
<1·0	27 (33%)	3 (20%)	9 (43%)	11 (37%)	4 (27%)	0·4941
≥1·0	54 (67%)	12 (80%)	12 (57%)	19 (63%)	11 (73%)	..
Platelet count, ×10⁹/L	212·2 (99·7)	202·9 (67·4)	213·5 (100·8)	206·8 (96·1)	230·5 (134·8)	0·8723
<100	0	0	0	0	0	..
≥100	81 (100%)	15 (100%)	21 (100%)	30 (100%)	15 (100%)	..
Haemoglobin, ng/mL	123·9 (12·0)	125·1 (13·5)	126·7 (13·4)	119·6 (12·8)	124·8 (9·1)	0·6494
C-reactive protein, mg/L	47·6 (41·8)	6·9 (5·4)	61·4 (39·6)	71·3 (39·8)	49·8 (42·4)	0·0051
Serum amyloid A protein, mg/L	213·5 (177·8)	143·3 (108·4)	257·6 (264·2)	216·6 (66·7)	NA	0·3300
Alanine aminotransferase, U/L	46·2 (29·5)	30·8 (8·9)	50·6 (24·8)	48·7 (33·1)	50·6 (37·7)	0·1629
Aspartate aminotransferase, U/L	40·8 (17·9)	30·2 (8·7)	47·7 (20·8)	42·7 (18·0)	37·8 (16·4)	0·0026
≤40	38 (47%)	11 (73%)	8 (38%)	12 (40%)	7 (47%)	0·1586
>40	43 (53%)	4 (27%)	13 (62%)	18 (60%)	8 (53%)	..
Total bilirubin, µmol/L	11·9 (3·6)	9·2 (0·6)	14·1 (4·3)	11·9 (3·9)	NA	0·4526
Albumin, g/L	32·9 (8·1)	NA	34·0 (9·3)	30·1 (2·8)	NA	0·5666
Glucose, mmol/L	6·4 (2·1)	6·4 (5·0)	5·2 (1·9)	6·8 (1·6)	NA	0·8713
Creatinine, µmol/L	75·4 (29·8)	63·7 (16·5)	68·0 (15·4)	115·4 (46·2)	58·4 (1·3)	0·1803
Prothrombin time, s	10·7 (0·9)	10·6 (0·9)	10·5 (0·4)	10·7 (1·0)	10·9 (1·6)	0·9022
Activated partial thromboplastin time, s	32·1 (7·6)	26·9 (3·9)	34·3 (6·7)	34·5 (13·1)	29·2 (2·4)	0·4814
Thrombin time, s	28·9 (8·4)	21·8 (5·4)	32·3 (8·2)	24·9 (7·6)	32·3 (7·9)	0·3169
Fibrinogen, g/L	1·5 (2·3)	0·7 (0·3)	1·92 (3·5)	2·3 (3·0)	0·3 (0·1)	0·7960
D-dimers, mg/L	6·5 (0·8)	6·5 (0·3)	6·9 (1·1)	5·8 (0·2)	NA	0·4940

(Table continues on next page)

	All patients (n=81)	Group 1 (n=15)	Group 2 (n=21)	Group 3 (n=30)	Group 4 (n=15)	p value*
(Continued from previous page)						
Comorbidities						
Any	21 (26%)	4 (27%)	5 (24%)	9 (30%)	3 (20%)	0·9397
Chronic pulmonary disease	9 (11%)	1 (7%)	3 (14%)	3 (10%)	2 (13%)	0·8945
Diabetes	10 (12%)	3 (20%)	2 (10%)	3 (10%)	2 (13%)	0·8005
Hypertension	12 (15%)	2 (13%)	1 (5%)	7 (23%)	2 (13%)	0·3571
Chronic renal failure	3 (4%)	0	0	3 (10%)	0	0·3101
Cardiovascular disease	8 (10%)	3 (20%)	1 (5%)	3 (10%)	1 (7%)	0·5494
Cerebrovascular disease	6 (7%)	1 (7%)	1 (5%)	3 (10%)	1 (7%)	0·9367
Malignancy	4 (5%)	1 (7%)	1 (5%)	2 (7%)	0	0·9148
Hepatitis or liver cirrhosis	7 (9%)	0	2 (10%)	3 (10%)	2 (13%)	0·6812

Data are mean (SD) or n (%). NA=not available. *Difference among groups 1–4.

Table: **Clinical characteristics and laboratory findings of patients with COVID-19 pneumonia**

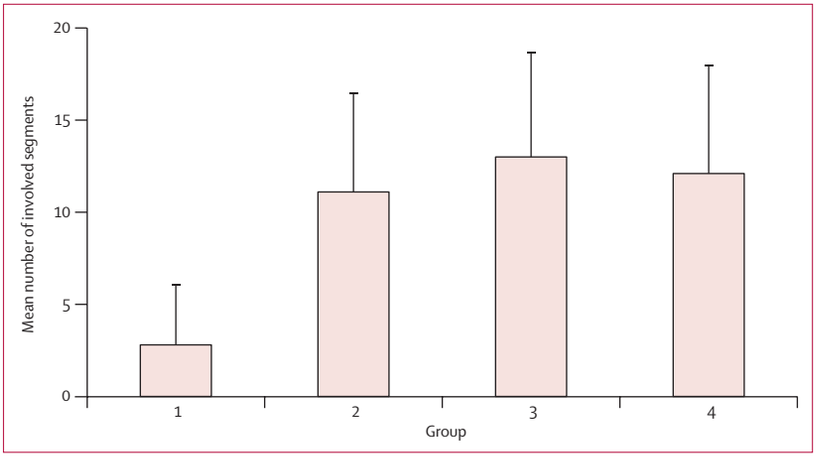

Figure 1: **Number of involved lung segments at various timepoints from symptom onset**
Bars show the mean number of involved lung segments on CT scans from patients in group 1 (scan before symptom onset; n=15), group 2 (scan ≤1 week after symptom onset; n=21), group 3 (scan >1 week to 2 weeks after symptom onset; n=30), and group 4 (scan >2 weeks to 3 weeks after symptom onset; n=15).

See Online for appendix 2

reconstructed images were transmitted to the workstation and picture archiving and communication systems (PACS) for multiplanar reconstruction post-processing.

Image interpretation

Images from cases seen at Union Hospital were analysed by two radiologists (HS [a senior thoracic radiologist with 30 years' experience] and XH [a radiology resident with 4 years' experience in interpreting chest CT images]). Images from cases seen at Wuhan Jinyintan Hospital were interpreted by two radiologists experienced in thoracic radiology (YF [12 years' experience] and NJ [10 years' experience]). All Digital Imaging and Communications in Medicine (DICOM) images from the CT studies were analysed without access to clinical or laboratory findings. The evaluators independently and freely assessed the CT features using both axial CT images and multiplanar reconstruction images. After separate evaluations, any disagreements were resolved by discussion and consensus. CT imaging features recorded from our cohort are summarised in the appendix 2 (p 4).

Follow-up chest CT

Follow-up chest CT scans were reviewed by two radiologists (HS and YF). The images were assessed and the evolution of lesions rated as either no significant change, resolution, or progression, compared with the previous chest CT from the same patient (appendix 2 p 4). Decisions were reached by consensus.

Statistical analysis

Analyses were done with SAS software version 9.4. Distribution normality was assessed using the Kolmogorov-Smirnov test. Normally distributed data were presented as mean (SD), non-normally distributed data as median (IQR), and categorical variables as frequency (%). CIs of proportions were calculated using the Clopper-Pearson method. Differences between groups were analysed by Fisher's exact test (for categorical data) or one-way ANOVA (for continuous data).

Role of the funding source

There was no funding source for this study.

Results

81 patients who were admitted to Wuhan Jinyintan hospital (n=49) or Union Hospital of Tongji Medical College (n=32) between Dec 20, 2019, and Jan 23, 2020, and who had confirmed COVID-19 pneumonia were retrospectively enrolled in our study. Epidemiologically, there were four main clusters of patients: 31 (38%) patients had direct exposure to Huanan seafood market, 15 (19%) were health-care workers who had close contact with patients at the hospital who had confirmed COVID-19 pneumonia, seven (9%) were familial clusters, and the remaining 28 (35%) did not have any obvious history of exposure. Patients were assigned to groups on

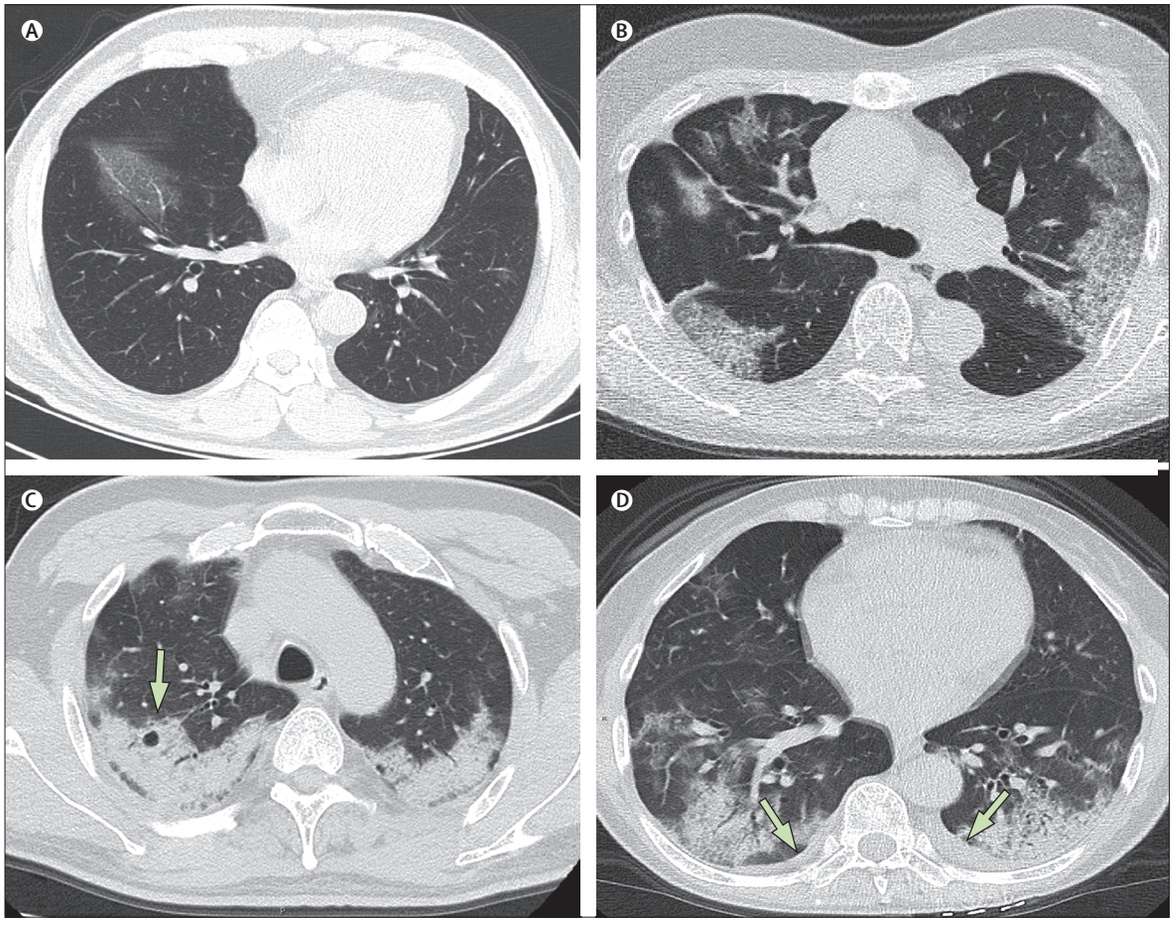

Figure 2: **Transverse thin-section CT scans in patients with COVID-19 pneumonia**
(A) 56-year-old man, day 3 after symptom onset: focal ground-glass opacity associated with smooth interlobular and intralobular septal thickening in the right lower lobes. (B) 74-year-old woman, day 10 after symptom onset: bilateral, peripheral ground-glass opacity associated with smooth interlobular and intralobular septal thickening (crazy-paving pattern). (C) 61-year-old woman, day 20 after symptom onset: bilateral and peripheral predominant consolidation pattern with a round cystic change internally (arrow). (D) 63-year-old woman, day 17 after symptom onset: bilateral, peripheral mixed pattern associated with air bronchograms in both lower and upper lobes, with a small amount of pleural effusion (arrows).

the basis of time between symptom onset and first CT scan: 15 (19%) patients (including health-care workers who had had close contact with patients with confirmed COVID-19 pneumonia) were assigned to group 1, 21 (26%) to group 2, 30 (37%) to group 3, and 15 (19%) to group 4.

The clinical characteristics and laboratory results of patients by group are summarised in the table (see appendix 2 [pp 1–3] for additional data). In the full cohort, the mean age was 49·5 years (SD 11; range 25–81), and there was no gender difference (42 [52%] men and 39 [48%] women). No significant differences in age (p=0·2778) or sex distribution (p=0·0871) between groups were identified. The most common symptoms at onset were fever (59 [73%] patients) and dry cough (48 [59%]). Other non-specific symptoms included dizziness (two [2%] patients), diarrhoea (three [4%]), vomiting (four [5%]), headache (five [6%]), and generalised weakness (seven [9%]). Among groups 2–4 (symptomatic patients), no significant differences in clinical parameters were found. Patients in group 1 had significantly lower mean concentrations of C-reactive protein (6·9 mg/L, p=0·0051) and aspartate aminotransferase (30·2 U/L, p=0·0026) than patients in the other three groups. Other laboratory findings did not significantly differ among groups, and the prevalence of underlying diseases was similar in all groups.

All patients had abnormal CT imaging features (appendix 2 pp 5–6). Although all lung segments can be involved, there was a slight predilection for the right lower lobe (225 (27%) of 849 affected segments among all patients). The mean number of segments involved among all groups was 10·5 (SD 6·4; range 1–18; appendix 2 pp 7–8), with significantly more segments involved in groups 2–4 (symptomatic patients) than group 1 (asymptomatic patients; p<0·0001). Group 3 had the highest mean number of involved segments (13·0 [5·7]; figure 1).

64 [79%] patients had bilateral lung involvement, 44 [54%] showed peripheral distribution, and 36 [44%] showed

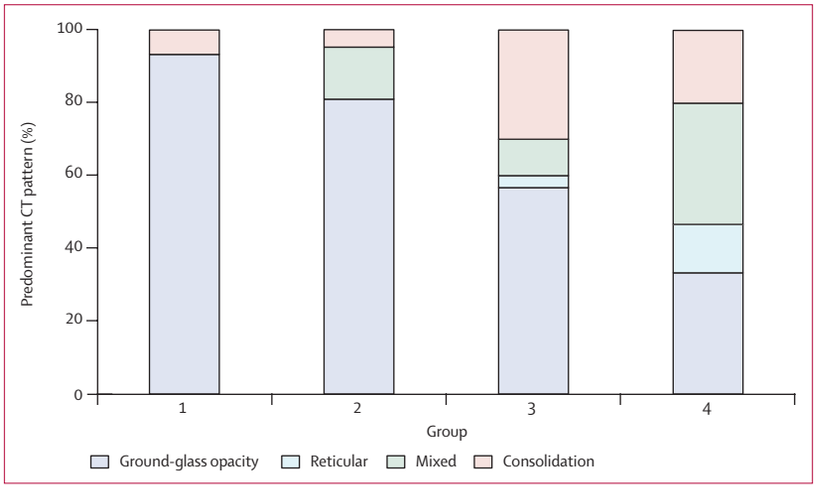

Figure 3: **Distribution of various patterns of lung changes on CT scans at various timepoints from symptom onset**

Stacked bars show the proportion of patients in whom the predominant CT pattern was ground-glass opacity, reticular, mixed, or consolidation. Patients were grouped by time from symptom onset: group 1 (scan before symptom onset; n=15), group 2 (scan ≤1 week after symptom onset; n=21), group 3 (scan >1 week to 2 weeks after symptom onset; n=30), and group 4 (scan >2 weeks to 3 weeks after symptom onset; n=15).

diffuse distribution of CT abnormalities (figure 2). The most common patterns seen on chest CT were ground-glass opacity (53 [65%] patients; figure 2A), in addition to ill-defined margins (66 [81%]), smooth or irregular interlobular septal thickening (28 [35%] patients; figure 2A), air bronchogram (38 [47%]; figure 2A, D), crazy-paving pattern (eight [10%]; figure 2B), and thickening of the adjacent pleura (26 [32%]). Less common CT findings were nodules (five [6%] patients), cystic changes (eight [10%]; figure 2C), bronchiolectasis (nine [11%]), pleural effusion (four [5%]; figure 2D), and lymphadenopathy (five [6%]). Tree-in-bud signs, masses, cavitation, and calcifications were not observed in our case series.

The typical pattern of CT imaging features from pre-clinical patients (group 1) comprised unilateral (nine [60%] patients), multifocal (eight [53%]), and ground-glass opacification (14 [93%]). Interlobular septal thickening, thickening of the adjacent pleura, nodules, round cystic changes, bronchiolectasis, pleural effusion, and lymphadenopathy were rarely observed in this group. In group 2 (first week after symptom onset), lesions quickly evolved to become bilateral (19 [90%] patients) and diffuse (11 [52%]), but remained predominantly of ground-glass opacity appearance (17 [81%]). Pleural effusion (one [5%]) and lymphadenopathy (three [14%]) were detected at this stage. In group 3 (second week after symptom onset), as the disease progressed, the ground-glass opacity pattern was still the predominant CT finding (17 [57%]); however, consolidation patterns (nine [30%]) were also noted. In group 4 (third week after symptom onset), ground-glass opacities (five [33%]) and reticular patterns (five [33%]) were the predominant imaging pattern (figure 3). Bronchiolectasis (two [13%]), thickening of the adjacent pleura (seven [47%]), pleural effusions (two [13%]), and lymphadenopathy (two [13%]) could also be seen at this stage (appendix 2 pp 5–6).

By Feb 8, 2020, 62 (77%) patients had been discharged, with a mean interval between symptom onset and discharge of 23·2 days (SD 6; range 12–41). 16 (20%) patients were still in hospital, and three (4%) patients had died (on days 12, 14, and 30, after hospital admission due to ARDS). Patient 1, who died on day 12 after admission, was a 60-year-old man with chronic pulmonary disease (tuberculosis). The CT scan obtained from this patient on day 8 after symptom onset showed extensive ground-glass opacities in both lungs, giving a white lung appearance (figure 4). The second patient who died (patient 2) was 73-year-old man who had had type 2 diabetes for several years, and showed progressive radiographic deterioration on CT scans taken on days 3, 7, and 11 after symptom onset. Patient 3, who died on day 30 after admission, was a 77-year-old man with hypertension, cardiovascular disease, and cerebrovascular disease. A CT scan showed mild pneumonia on day 5 after symptom onset in this patient (figure 5A), and two follow-up CT scans 10 days and 15 days later revealed rapid progression of the lung lesions with bilateral pleural effusions (figure 5B, C).

Follow-up CT images were obtained from 57 (70%) patients (36 from Wuhan Jinyintan hospital, and 21 from Union Hospital). 23 of these patients had two CT scans, 19 had three scans, and 15 had four scans available. Four patterns of evolution throughout the series of CT scans were observed among these 57 patients: initial progression to peak level, followed by radiographic improvement (type 1), seen in 26 (46%) patients (figure 6), of whom 24 (92%) patients were discharged from hospital (median stay 25 days [IQR 20–27]); radiographic deterioration (type 2), seen in 18 (32%) patients (figure 5), of whom two (11%) died (patients 2 and 3); radiographic improvement (type 3), seen in eight (14%) patients, of whom five (63%) were discharged from hospital (median stay 19 days [IQR 11–25]); and unchanged radiographic appearance (type 4), seen in five (9%) patients, all of whom were still in hospital at the cutoff date (Feb 8).

Discussion

The Coronaviridae family of viruses includes six previously known human-infecting coronaviruses, which are enveloped, non-segmented, positive-sense RNA viruses that are broadly distributed in humans and other mammals.[13] Although four of these coronaviruses cause only mild respiratory symptoms similar to the common cold, epidemics caused by two betacoronaviruses, SARS-CoV in 2002[14,15] and MERS-CoV in 2012, involved more than 8000 patients and 1000 patients, respectively,[16,17] with high mortality rates (10% for SARS-CoV and 37% for MERS-CoV). The novel coronavirus SARS-CoV-2 is the seventh member of the Coronaviridae family known to infect humans. The mortality rate of COVID-19 so far is

lower than that of SARS or MERS coronavirus diseases; however, SARS-CoV-2 is highly infectious and could be a significant health threat.

In our study, the predisposing conditions for COVID-19 pneumonia tended to be old age and medical comorbidities (such as chronic pulmonary disease, diabetes, and other chronic diseases), similar to previous viral infections such as influenza H7N9.[18,19] There was no obvious predilection for males or females in our cohort. However, another study reported that 30 (73%) of 41 infected patients were men.[5] This discrepancy might be due to the differences in demographic features and small cohorts. By Feb 8, 2020, three patients in our study had died, representing a mortality rate of around 4%. All deaths occurred in men older than 60 years who had underlying diseases, consistent with previous reports.[5] Thus, old age, male sex, and presence of comorbidities might be risk factors for poor prognosis.

Fever, cough, and dyspnoea were the most common symptoms in patients with COVID-19 pneumonia, consistent with the manifestation of lower respiratory tract infections. By contrast, upper respiratory tract symptoms were less common in these patients, indicating that the cells targeted by the virus might be located in the lower airway.[5] Other non-specific symptoms included dizziness, diarrhoea, vomiting, headache, and generalised weakness, which occurred in around 2–9% of patients. Notably, 15 cases of asymptomatic infection were discovered on the basis of abnormal lung findings on CT scans, suggesting that chest CT scans or serum antibody tests should be done in asymptomatic high-risk individuals with a history of exposure to patients with COVID-19 pneumonia to facilitate early identification of the disease.

In our cohort, leukocytosis was detected in 26 (32%) patients and lymphocytosis in 54 (67%) patients. Concentrations of C-reactive protein and serum amyloid A protein were elevated in most patients, as observed in previous betacoronavirus infections.[10,11,20] In the subgroup of asymptomatic patients (group 1), concentrations of C-reactive protein (6·9 mg/L) and aspartate aminotransferase (30·2 U/L) were lower than those in symptomatic patients.

The mean number of involved lung segments in our cohort was 10·5, with the right lower lobes most commonly affected. This finding is similar to those of a previous radiological study of patients with H7N9 influenza infection.[21] This finding might be due to the anatomical structure of the trachea and bronchi: as the right bronchus is short and straight, the causative virus might tend to favour this location.

The extent of disease on CT scans showed a marked increase from the subclinical period through the first and second weeks after symptom onset, then decreased gradually in the third week. A previous study showed that the median time from onset of symptoms to mechanical ventilation was 10·5 days (IQR 7·0–14·0) and to intensive care unit admission was 10·5 days (8·0–17·0).[5] Thus, our findings indicate that the radiological evolution of COVID-19 pneumonia is consistent with the clinical course of the disease.

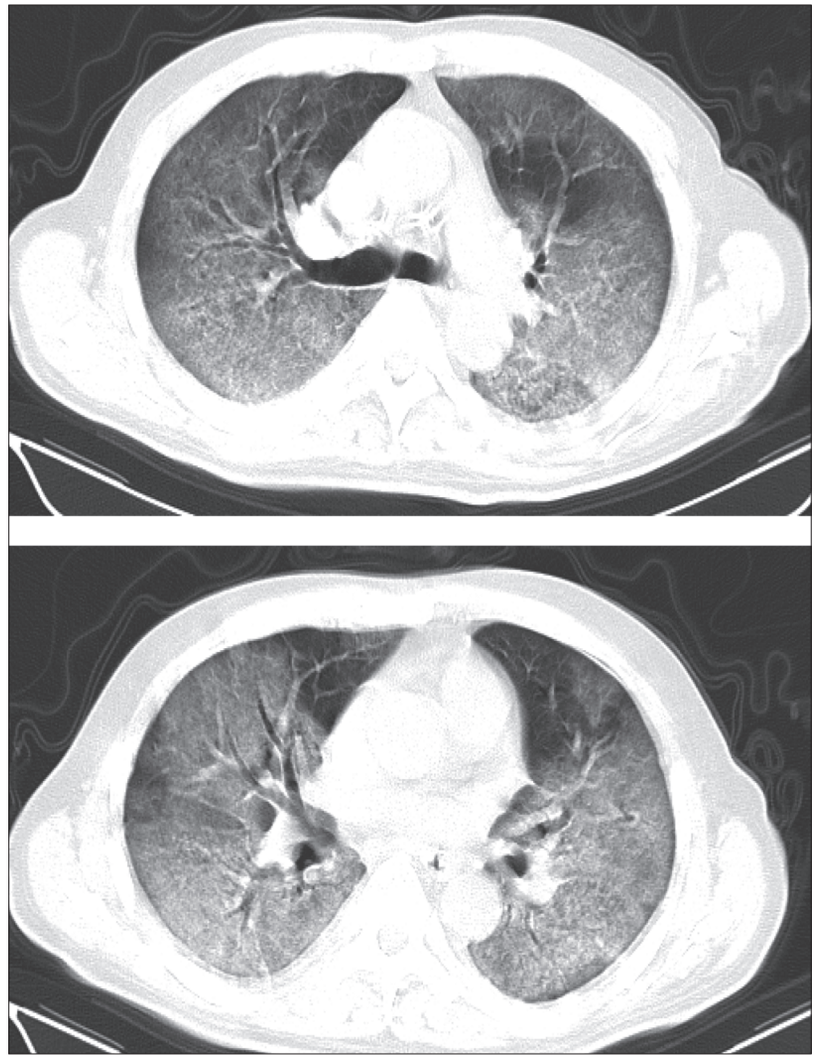

Figure 4: **Transverse CT scans from a 60-year-old man (day 8 after symptom onset)**
Selected images from CT scans at different levels. Extensive ground-glass opacities can be seen in both lungs, involving almost the entire lower lobes, and most of the upper lobes and right middle lobe, giving a white lung appearance, with air bronchograms. The patient died 4 days after this scan.

Most patients in our cohort showed bilateral lung involvement, with lesions mainly located peripherally and subpleurally with diffuse distribution. The predominant pattern was ground-glass opacity, with ill-defined margins, air bronchograms, smooth or irregular interlobular or septal thickening, and thickening of the adjacent pleura. These imaging characteristics are non-specific and bear some resemblance to those of SARS-CoV[22–24] and MERS-CoV infections.[25,26] However, unlike SARS-CoV infections, some patients in our study presented with pleural effusion, lymphadenopathy, and round cystic changes on CT. Previous studies showed that

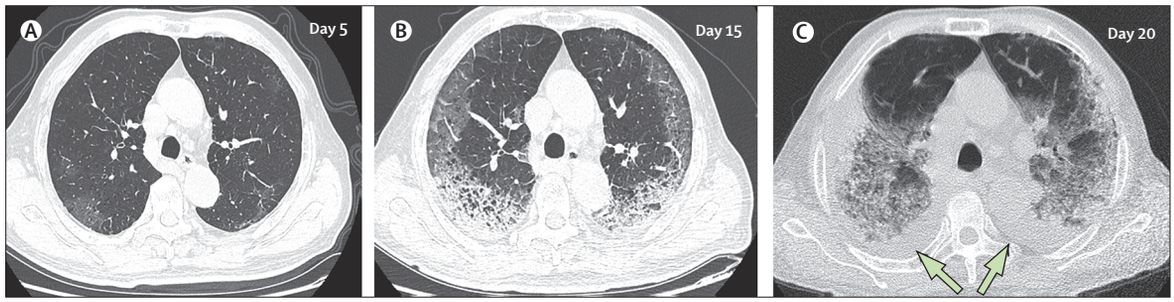

Figure 5: **Transverse thin-section serial CT scans from a 77-year-old man**
(A) Day 5 after symptom onset: patchy ground-glass opacities affecting the bilateral, subpleural lung parenchyma. (B) Day 15: subpleural crescent-shaped ground-glass opacities in both lungs, as well as posterior reticular opacities and subpleural crescent-shaped consolidations. (C) Day 20: expansion of bilateral pulmonary lesions, with enlargement and denser pulmonary consolidations and bilateral pleural effusions (arrows). The patient died 10 days after the final scan.

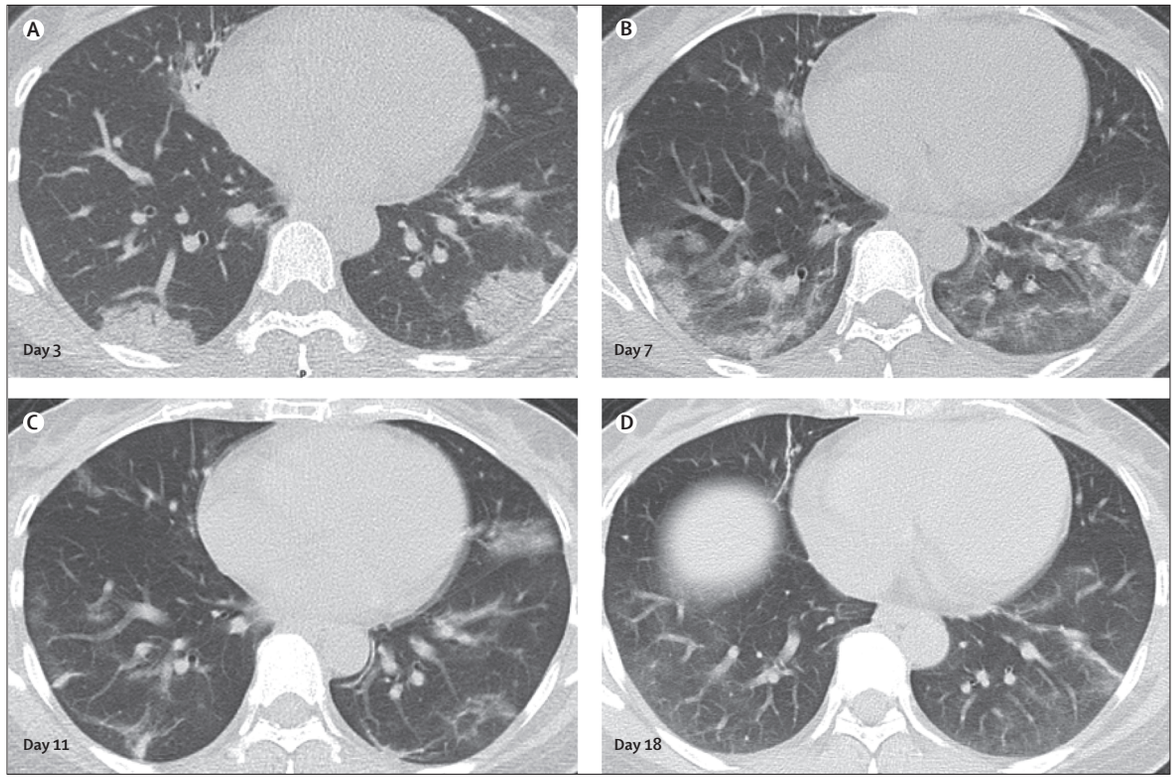

Figure 6: **Transverse thin-section serial CT scans from a 42-year-old woman**
(A) Day 3 after symptom onset: multifocal consolidations affecting the bilateral, subpleural lung parenchyma. (B) Day 7: the lesions had increased in extent and the density became heterogeneous, with internal bronchovascular bundle thickening. (C) Day 11: previous opacifications being dissipated into ground-glass opacities and irregular linear opacities. (D) Day 18: further resolution of the lesions. The patient was discharged from hospital 2 days after the final scan.

the presence of pleural effusion in patients infected with MERS-CoV or avian influenza H5N1 was a poor prognostic indicator.[25,27,28] Similarly, in one patient who died in our study (patient 3), a follow-up CT scans showed that he had developed bilateral pleural effusion. On the other hand, lymphadenopathy has also been seen in cases of H5N1 infection,[28] which can present as a rapidly progressive pneumonia that results in ARDS. Round cystic changes on CT might be associated with the process of resorption of consolidation; which might be explained by the infection causing damage to the alveolar walls and leading to pneumatoceles. Other findings included intralobular or interlobular septal thickening, and a crazy-paving pattern. However, none of the CT features of COVID-19 seem to be specific or diagnostic, and COVID-19 pneumonia shares CT features with other non-infectious conditions that present as subpleural air-space disease. For example, patients with bronchiolitis obliterans with organising pneumonia[29,30] often show nodules (32%),[29] lymphadenopathy (13%),[30] and pleural effusion (20%).[30] These findings were present, albeit with lower frequency, among our patients with COVID-19

pneumonia (nodules 6%, lymphadenopathy 13%, pleural effusion 5%). However, tree-in-bud signs, masses, cavitations, and calcifications, often suggestive of bacterial or chronic infections, were absent in our study.

The typical pattern of CT images in subclinical patients (group 1) was unilateral, multifocal, predominantly ground-glass opacities. In the first week after symptom onset (group 2), lesions quickly evolved to bilateral, diffuse disease, with a relative decrease in the frequency of ground-glass opacities and a transition to consolidation and mixed-pattern development. Pleural effusion and lymphadenopathy were also detected in group 2. Subsequently, ground-glass opacities continued to decrease in frequency throughout the second week after symptom onset (group 3), while consolidation became the second most common pattern. A reticular pattern associated with bronchiolectasis and irregular interlobular or septal thickening were also noted to increase progressively from the second week. These findings indicated the appearance of interstitial changes, suggesting the development of fibrosis. However, since the natural history of COVID-19 pneumonia is yet to be fully explored, it is too early to label these lung changes as irreversible fibrosis. As the disease progressed in the third week after symptom onset, consolidation and mixed patterns became more common, while ground-glass opacities decreased further. Bronchiolectasis, thickening of the adjacent pleura, and pleural effusion mainly appeared at this stage.

Serial CT imaging of patients could help to continuously monitor disease changes. Follow-up CT showed progression or improvement of lung lesions during treatment, sensitively reflecting therapeutic effects, and these changes might be related to outcomes in such patients. The most common pattern of evolution throughout series of CT scans in this study was initial progression to a peak level, followed by radiographic improvement (type 1), and most of these patients were subsequently discharged. In addition, most patients who showed a pattern of radiographic improvement across several scans (type 3) were discharged from hospital. Thus, a type 1 or type 3 disease course might be associated with favourable outcomes. On the other hand, progressive radiographic deterioration despite medical treatment seems to be associated with poor prognosis, with two deaths in our study occurring among the 18 patients with the type 2 pattern.

Our study had several limitations. First, at the time of data collection, nucleic acid testing for the diagnosis of SARS-CoV-2 infection had not yet been introduced at Union Hospital, and 33 patients were therefore diagnosed clinically on the basis of WHO criteria.[12] However, all these cases were confirmed by nucleic acid testing when kits became available later. Second, we compared imaging patterns between four groups of different time intervals from the onset of symptoms, which does not account for potential individual variations. Third, because of the short time for case collection, follow-up CT scans were available for only 57 patients, around 40% of whom had only two CT scans. Although we have outlined the main patterns of evolution seen on CT imaging in patients with COVID-19 pneumonia, long-term radiological follow-up is needed to confirm our findings. Finally, as lung biopsy specimens were not available in this study, the relationship between radiological and histopathological findings remains to be investigated. Therefore, other potential causes of ground-glass opacity, such as pulmonary oedema and haemorrhage, cannot be estimated.

In conclusion, COVID-19 pneumonia tends to manifest on lung CT scans as bilateral, subpleural, ground-glass opacities with air bronchograms, ill-defined margins, and a slight predominance in the right lower lobe. Abnormal lung CT findings can be present even in asymptomatic patients, and lesions can rapidly evolve into a diffuse ground-glass opacity predominance or consolidation pattern within 1–3 weeks after onset of symptoms, peaking at around 2 weeks after onset. Old age, male sex, underlying comorbidities and progressive radiographic deterioration on follow-up CT might be risk factors for poor prognosis in patients with COVID-19 pneumonia.

Contributors

HS, YF, and CZ conceived and designed the study. XH and NJ contributed to the literature search. XH, NJ, JG, YF, and CZ contributed to data collection. HS, XH, and YC contributed to data analysis. YC and OA contributed to data interpretation. HS, XH, NJ and YF contributed to the figures. HS, XH, NJ, and OA contributed to writing of the report.

Declaration of interests

We declare no competing interests.

Acknowledgments

We thank all our colleagues who helped us during the current study. We greatly appreciate the kind assistance of Xiaoming Yang (Radiology, University of Washington, Seattle, WA, USA) and Hanping Wu (Radiology, University of Michigan, Ann Arbor, MI, USA) in editing and revising the manuscript, as well as Hongwei Jiang (Epidemiology & Biostatistics, Tongji Medical College, Huazhong University of Science and Technology, Wuhan, China) for his assistance in statistical analysis. We are also grateful to the many front-line medical staff for their dedication in the face of this outbreak, despite the potential threat to their own lives and the lives of their families.

References

1 WHO. Novel coronavirus—China. Jan 12, 2020. https://www.who.int/csr/don/12-january-2020-novel-coronavirus-china/en/ (accessed Feb 12, 2020).

2 WHO. Coronavirus disease (COVID-19) outbreak. 2020. https://www.who.int/emergencies/diseases/novel-coronavirus-2019 (accessed Feb 15, 2020).

3 Xu X, Chen P, Wang J, et al. Evolution of the novel coronavirus from the ongoing Wuhan outbreak and modeling of its spike protein for risk of human transmission. *Sci China Life Sci* 2020; published online Jan 21. DOI:10.1007/s11427-020-1637-5.

4 Tan W, Zhao X, Ma X, et al. Notes from the field: a novel coronavirus genome identified in a cluster of pneumonia cases—Wuhan, China 2019–2020. *China CDC Weekly* 2020; **2:** 61–62.

5 Na Z, Ding Z, Wen W, et al. Clinical features of patients infected with 2019 novel coronavirus in Wuhan, China. *Lancet* 2020; **395:** 497–605

6 WHO. Novel coronavirus—Thailand (ex-China). Jan 14, 2020. https://www.who.int/csr/don/14-january-2020-novel-coronavirus-thailand/en/ (accessed Feb 8, 2020).

7 WHO. Novel coronavirus—Japan (ex-China). Jan 17, 2020. https://www.who.int/csr/don/17-january-2020-novel-coronavirus-japan-ex-china/en/ (accessed Jan 19, 2020).

8 WHO. Novel coronavirus—Republic of Korea (ex-China). Jan 21, 2020. https://www.who.int/csr/don/21-january-2020-novel-coronavirus-republic-of-korea-ex-china/en/ (accessed Jan 23, 2020).

9 US Centers for Disease Control and Prevention. First travel-related case of 2019 novel coronavirus detected in United States. Jan 21, 2020. https://www.cdc.gov/media/releases/2020/p0121-novel-coronavirus-travel-case.html (accessed Feb 15, 2020).

10 Tsang KW, Ho PL, Ooi GC, et al. A cluster of cases of severe acute respiratory syndrome in Hong Kong. *N Engl J Med* 2003; **348:** 1977–85.

11 Assiri A, Al-Tawfq JA, Al-Rabeeah AA, et al. Epidemiological, demographic, and clinical characteristics of 47 cases of Middle East respiratory syndrome coronavirus disease from Saudi Arabia: a descriptive study. *Lancet Infect Dis* 2013; **13**: 752–61.

12 WHO. Clinical management of severe acute respiratory infection when novel coronavirus (2019-nCoV) infection is suspected: interim guidance. Jan 28, 2020. https://www.who.int/docs/default-source/coronaviruse/clinical-management-of-novel-cov.pdf (accessed Feb 15, 2020).

13 Richman DD, Whitley RJ, Hayden FG, eds. Clinical virology, 4th edn. Washington: ASM Press, 2016.

14 Ksiazek TG, Erdman D, Goldsmith CS, et al. A novel coronavirus associated with severe acute respiratory syndrome. *N Engl J Med* 2003; **348:** 1953–66.

15 Kuiken T, Fouchier RAM, Schutten M, et al. Newly discovered coronavirus as the primary cause of severe acute respiratory syndrome. *Lancet* 2003; **362:** 263–70.

16 de Groot RJ, Baker SC, Baric RS, et al. Middle East respiratory syndrome coronavirus (MERS-CoV): announcement of the Coronavirus Study Group. *J Virol* 2013; **87:** 7790–92.

17 Zaki AM, van Boheemen S, Bestebroer TM, Osterhaus AD, Fouchier RA. Isolation of a novel coronavirus from a man with pneumonia in Saudi Arabia. *N Engl J Med* 2012; **367:** 1814–20.

18 Liu S, Sun J, Cai J, et al. Epidemiological, clinical and viral characteristics of fatal cases of human avian influenza A (H7N9) virus in Zhejiang Province, China. *J Infect* 2013; **67:** 595–605.

19 Chen X, Yang Z, Lu Y, Xu Q, Wang Q, Chen L. Clinical features and factors associated with outcomes of patients infected with a novel influenza A (H7N9) virus: a preliminary study. *PLoS One* 2013; **8:** e73362.

20 Lee N, Hui D, Wu A, et al. A major outbreak of severe acute respiratory syndrome in Hong Kong. *N Engl J Med* 2003; **348:** 1986–94.

21 Wang Q, Zhang Z, Shi Y, Jiang Y. Emerging H7N9 influenza A (novel reassortant avian-origin) pneumonia: radiologic findings. *Radiology* 2013; **268:** 882–89.

22 Müller NL, Ooi GC, Khong PL, Nicolaou S. Severe acute respiratory syndrome: radiographic and CT findings. *AJR Am J Roentgenol* 2003; **181:** 3–8.

23 Wong KT, Antonio GE, Hui DS, et al. Thin-section CT of severe acute respiratory syndrome: evaluation of 73 patients exposed to or with the disease. *Radiology* 2003; **228:** 395–400.

24 Zhao Z, Liang C, Zhang J, Zhang R, He H. Clinical and imaging findings in patients with severe acute respiratory syndrome. *Chin Med J (Engl)* 2003; **116:** 1104–05.

25 Das KM, Lee EY, Enani MA, et al. CT correlation with outcomes in 15 patients with acute Middle East respiratory syndrome coronavirus. *AJR Am J Roentgenol* 2015; **204:** 736–42.

26 Ajlan AM, Ahyad RA, Jamjoom LG, Alharthy A, Madani TA. Middle East respiratory syndrome coronavirus (MERS-CoV) infection: chest CT findings. *AJR Am J Roentgenol* 2014; **203:** 782–87.

27 Das KM, Lee EY, Al Jawder SE, et al. Acute Middle East respiratory syndrome coronavirus: temporal lung changes observed on the chest radiographs of 55 patients. *AJR Am J Roentgenol* 2015; **205:** W267–74.

28 Qureshi NR, Hien TT, Farrar J, Gleeson FV. The radiologic manifestations of H5N1 avian influenza. *J Thorac Imaging* 2006; **21:** 259–64.

29 Ujita M, Renzoni EA, Veeraraghavan S, Wells AU, Hansell DM. Organizing pneumonia: perilobular pattern at thin-section CT. *Radiology* 2004; **232:** 757–61.

30 Travis WD, Costabel U, Hansell DM, et al. An official American Thoracic Society/European Respiratory Society statement: update of the international multidisciplinary classification of the idiopathic interstitial pneumonias. *Am J Respir Crit Care Med* 2013; **188:** 733–48.